SIF BANDHOLTZ HANSEN · SØREN SINDBÆK · MORTEN SØVSØ · SARAH CROIX
GRY HOFFMANN BARFOD

ALL UNDER ONE ROOF –
CHEMICAL AND SR ISOTOPE ANALYSIS OF GLASS FROM A VIKING AGE PIT HOUSE AT RIBE

Through Antiquity and the Early Middle Ages three main glass types were in use in western Eurasia. The earliest glass production centered in the Mesopotamia area around BC 1500 was plant ash glass made from mixing ash from halophytic (salt-loving) plants with quartz (SiO_2). In the 2nd century BC, a new type, natron glass, appeared and became the dominant glass type in the Mediterranean area during most of the 1st millennium AD whilst plant ash production still continued in the east. Natron glass was produced at large-scale factories along the Syria-Palestinian coast or in Egypt until around the end of the 7th century AD, when the production ceased and plant ash glass again spread from the East to the Levant[1]. Once natron supplies stopped, production of plant ash glass presumably could not keep up with demand due to the limited geographical extent of halophytic plants and a new glass type based on wood ash mixed from quartz appeared presumably in the western part of the Carolingian Empire around AD 780[2]. Because wood was not restricted to saline areas, as was the case with both natron and halophytic plants, wood ash glass production soon became widespread (e. g. France, England and Germany).

The raw materials for these three main glass types are distinct and the growing range of analytical methods applied to the study of ancient and medieval glass increasingly enables researchers to trace the »flow of glass from the production sites to the smallest workshop« through trace element and isotopic signatures[3]. The »smallest workshops« – tertiary production sites where glass was reworked on a minor scale – are becoming viable targets for analysis as major patterns of glass types and supply are better understood, and as more precise analytical methods enables researchers to trace mixing and processing.

In this study, we trace the travels of glass north via trade routes to a house dated to the 9th century in the trading emporium of Ribe. The study involves chemical characterization of 16 glass fragments found in the remains of a sunken-featured building investigated in 2014-2015 at Rosen Allé, Ribe. We use major and trace elements as well as Sr isotopic ratios to identify the glass types thus revealing critical information about trading to Ribe during the 9th century – and about post-depositional disturbances in archaeological sequences.

SAMPLE MATERIAL

The samples were collected from a single sunken-featured building (feature K4) investigated at Rosen Allé, Ribe, during the first and the second of three archaeological campaigns conducted between 2014 and 2016 by Aarhus University and Museum of Southwest Jutland.

The 2014-2016 Rosen Allé investigations covered an area of ca. 2400 m² that lay in direct continuation of an excavation in 1989[4]. The site presents a long continuity of use, from the late Iron Age until today, and the objective of the new campaigns was to investigate the outskirts of the Viking Age emporium, to the

In: Michael Dodt · Andreas Kronz · Bente S. Majchczack · Sebastian Messal (Hrsg.), Glas als Fernhandelsprodukt im frühen Mittelalter – Köln und der europäische Norden. RGZM – Tagungen 46 (Mainz 2022).
DOI: http://doi.org/10.11588/propylaeum.1105.c15174

north-east of the settlement centre, with a particular focus on the 8th-early 9th century pre-Christian burials and the late 9th-10th century earthworks. Probably contemporary with the early earthworks, a number of settlement structures have been identified in the form of sunken-featured buildings and post-built constructions. Among these, four sunken-featured buildings were investigated, two of which were dated with a coin-based *terminus post quem* (one by a Carolingian »Christiana Religio« coin, between 822/823-840; another by two cuttings of Samanid dirhems, ca. 890-950). Both the artefact material associated with these features and their stratigraphic relations to older graves and younger settlement features provide a broader chronological frame-work ranging to the mid-9th-10th centuries. While the level of activity at Rosen Allé appears rather low in comparison with the profusion of finds and the thick accumulation of stratified deposits at the market-site, its character still echoes that of the heart of the emporium, with evidence for various types of craft production as well as imported goods such as Badorf pottery and basalt quernstone from the Rhineland or whetstones from Norway.

The sunken-featured building K4 consisted in a large cutting, oval in shape, ca. 4m long and ca. 20cm deep. At each end of the long axis, two roof-bearing posts were observed. This construction is similar to hundreds of Viking Age sunken-featured buildings documented in southern Scandinavia, although its size lies at the larger end of the scale. It was investigated over two seasons, the northern half in 2014, the southern half in 2015. Its fill was composed of fairly homogenous, dark-brown humic sand with bits of charcoal, which had a slightly lighter colouration in its lower part. Despite careful excavation, no floor deposit could be recorded – presumably due to extensive bioturbation including animal burrowing as observed in the field. The bottom of the building pit was flat and fairly even. Finds of loom weights and spindle whorls *in situ* indicate that K4 probably was used for textile production. After being abandoned it was filled in and the homogenous appearance of the fill layer is a result of subsequent bioturbation. The entire fill was sieved with a 4mm mesh to retrieve smaller artefacts. The large majority of the finds relates to the fill layers and consisted of Viking Age ceramic sherds (semi-spherical vessels, local grey ware). They also included fragments of amber and (purple) whetstone. There was a fair amount of intrusive material, including medieval ceramic, fragments of tiles and bricks, and even some early modern material in the form of window glass and clay pipe fragments. Thus, the artefact material retrieved from the fill of sunken-featured building K4 attests to activity conducted in the building itself, mainly textile production, but also to secondary deposition in the Viking Age and later disturbances caused by bioturbation combined with the occupation of the site in the following centuries.

The building yielded a number of glass beads as well as fragments of vessel glass and other glass objects. Some of these were probably intrusive from bioturbation, such as the window glass mentioned above. **Table 1** provides short descriptions, pictures, colours and types of the glass fragments. Letters after find numbers distinguish individual pieces collected from the same find context (= with identical find numbers) and refer to sherd colours (**tab. 1**). The glass artefacts include chips (2), beads (5), and unidentified fragmented pieces (9).

METHODOLOGY

The 16 glass samples were analysed for major and minor elements by electron microprobe (EMP), for trace elements by laser ablation (LA) ICP-MS and for Sr isotopic composition by Multi-Collector (MC) ICP-MS. For EMP and LA-ICP-MS analysis, small (1 mm × 1 mm) fragments were chipped from the glass samples, mounted in epoxy and polished. Care was taken to avoid glass surfaces given the well-known Na loss at surfaces due to the exposure to surrounding sediments[5].

Sample	Cat. No.	Picture	Color	Type of glass	Glass type
Roman glass					
G1	200212264DG[1] x262	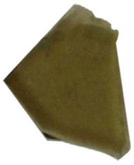	Greenish	Glass sherd	Sb-Mn Roman glass
G2	200212679 x221		Blue, opaque	Glass fragment, tesserae	Mn Roman glass
G3	200212391B[2] x282		Blue, opaque	Glass fragment, tesserae	Mn Roman glass
Plant ash glass					
G4	200212267 x262		Blue	Bead	Plant ash glass
G5	200212677 x221		Blue	Bead	Plant ash glass
Early wood ash glass					
G6	200212680 x221		Green	Bead	Early Wood ash
G7	200212955 x247		Turquoise	Bead	Early Wood ash
G8	200212685 x221		Turquoise	Bead	Early Wood ash

Tab. 1 Overview of glass types, colours and typology from pit house K4, SJM 348, Ribe. – [1] DG = Dark green, [2] B = Blue, [3] LG = Light green, [4] T = Transparent. – (Table Museum of Southwest Jutland).

Sample	Cat. No.	Picture	Color	Type of glass	Glass type
Wood ash glass					
G9	200212956 x247		Greenish	Glass sherd	Wood ash
Wood ash lime glass					
G10	200212264LG[3] x262		Light greenish	Glass sherd	Wood ash lime glass
G11	200212041 x066		Greenish	Glass sherd	Wood ash lime glass
G12	200212927 x262		Greenish	Glass sherd	Wood ash lime glass
Mixed Alkali glass					
G13	200212483 x102	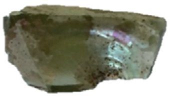	Greenish	Glass sherd	Mixed alkali glass
G14	200212957 x247		Greenish	Glass sherd	Mixed alkali glass
G15	200272281 x386	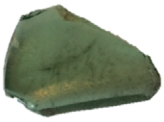	Greenish	Glass sherd	Mixed alkali glass
Modern-day glass					
G16	200212391T[4] x282		Colourless	Thick glass piece	Synthetic soda glass

Tab. 1 (continued).

Electron Microprobe (EMP)

Samples were analysed at the Department of Geoscience at Aarhus University on a JEOL JXA-8600 Superprobe by energy-dispersive spectroscopy (EDS). Calibrations were done using natural minerals (rhodonite [Mn], hematite [Fe], Al_2O_3 [Al], jadeite [Na], sanidine [K], MgO [Mg], quartz [Si] and apatite [P]) and analytical settings were acceleration voltage of 15 kV, beam current at 10 nA, and 20 sec analysis time. Throughout the session, Corning glass standard B from Corning Museum of glass was analysed repeatedly to monitor reproducibility and accuracy (n = 16). This showed reproducibilities better than 55 % for concentrations ranging from 0.05 wt % to 1.10 wt % (Cl, MnO, FeO, and P_2O_5), 16 % for concentrations between 1.15 wt % and 1.30 wt % (MgO and K_2O) and better than 6.5 % for concentrations above 1.30 wt %. Data for the glass samples in **table 2** and **figure 1** represent means of eight measurements. The accuracy of the measurements was also estimated from the Corning B glass standard by comparing our obtained values with the recommended analyses summarized by Adlington (2017). This showed accuracies for concentrations ranging from 0.10 wt % to 1.30 wt % to be better than 34 % (with the exception of Cl which is higher; **tab. 2**). Concentrations above 1.3 wt % had accuracies better than 12 %. The relatively high deviations for low concentration elements such as MgO, K_2O and Al_2O_3 from known values meant that we chose to use LA-ICP-MS data for these elements in plots and interpretations.

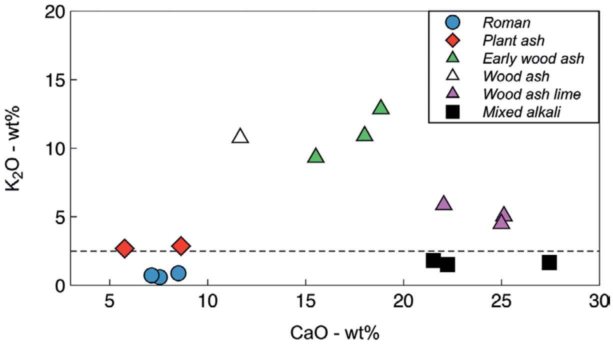

Fig. 1 Variation diagram of CaO (wt %) and K_2O (wt %) for the glass groups from house K4 in Ribe. For samples with CaO below 10 wt %, punctuated line at 2.5 wt % separates natron glass (below line) from plant ash glass (above line). Values from **tab. 3**. – (Diagram Museum of Southwest Jutland).

Laser Ablation (LA) ICP-MS

Trace element analyses were done at the AGiR (Aarhus Geochemistry and Isotope Research) platform on an Agilent 7900 quadrupole ICP-MS coupled to a Resonetics 193 nm laser ablation instrument. Laser settings included laser energy at 80 mJ, 60 um spot size, 10 Hz repetition rate and acquisition time of 71 sec. Data reductions were done with Iolite Software using USGS glass standard GSE-G1 as calibration standard and by matching Si counts for samples to the SiO_2 concentrations obtained from EMP analyses. Repeated analysis of USGS glass standard GSD-G1 was within 5 % of known values for most elements (n = 18). Sample analyses listed in **table 3** and presented in **figure 2** represent means of five repeats.

Multi-Collector (MC) ICP-MS

About 50 mg glass was weighed out and strontium separated on Sr spec using conventional elution scheme with nitric acid dilutions and analysed by Nu Plasma II at AGiR[6]. This was repeated three months later for separate fragments of each sample and Corning B standard. Mass fractionation on $^{87}Sr/^{86}Sr$ ratios was corrected to $^{86}Sr/^{88}Sr = 0.1194$ and interferences of ^{87}Rb on ^{87}Sr and ^{86}Kr on ^{86}Sr were monitored by measuring signal on masses 85 (= ^{85}Rb) and 84 (= $^{84}Kr + ^{84}Sr$), respectively. These signals were less than a few mV. The SRM 987 standard was run after every four samples and the $^{87}Sr/^{86}Sr$ ratios of the samples normalized to an accepted value of 0.710248 for SRM 987. Normalized $^{87}Sr/^{86}Sr$ ratios of 0.703473 (± 0.000014) were obtained for standards USGS standards BHVO-2, which is within uncertainty of $^{87}Sr/^{86}Sr$ value for BHVO-2 of 0.703481 (± 0.000016)[7]. Corning B yielded $^{87}Sr/^{86}Sr$ ratios of 0.708932 (± 0.000019)[8]. **Table 4** shows the mean of results obtained for the samples taken through chemistry twice three months apart.

Glass Type	Cat. No.	Na_2O	MgO	Al_2O_3	SiO_2	P_2O_5	Cl	K_2O	CaO	FeO	MnO	Total
Roman glass												
G1	212264DG[1]	16.1 (5)	1.23 (27)	3.55 (27)	70.5 (8)	0.43 (25)	0.23 (4)	1.05 (14)	7.58 (28)	0.59 (20)	0.46 (19)	102
G2	212679	16.7 (6)	0.98 (23)	3.01 (30)	66.8 (4)	0.44 (23)	0.29 (4)	0.71 (14)	7.15 (32)	0.74 (13)	0.71 (31)	97.6
G3	212391B[2]	15.7 (3)	1.07 (23)	3.05 (27)	63.3 (1)	0.47 (28)	0.22 (4)	0.80 (12)	6.79 (51)	0.70 (22)	0.42 (20)	92.5
Plant ash glass												
G4	212267	15.1 (2)	5.85 (16)	2.33 (39)	66.0 (4)	0.44 (18)	0.19 (4)	2.83 (12)	5.07 (22)	1.29 (39)	1.49 (22)	101
G5	212677	14.9 (2)	4.36 (19)	2.74 (24)	66.1 (4)	0.61 (28)	0.27 (2)	3.01 (14)	7.44 (19)	0.78 (13)	0.16 (8)	100
Early wood ash glass												
G6	212680	1.08 (25)	5.48 (37)	3.75 (27)	54.0 (5)	2.73 (24)	0.07 (2)	13.2 (2)	16.3 (6)	0.90 (20)	1.69 (24)	99.1
G7	212955	0.81 (22)	4.33 (30)	3.29 (30)	61.5 (9)	3.23 (30)	0.08 (3)	11.2 (3)	15.3 (4)	0.71 (14)	0.60 (32)	101
G8	212685	1.00 (26)	4.72 (22)	3.00 (30)	58.8 (11)	2.92 (21)	0.06 (3)	9.08 (36)	12.7 (6)	0.52 (13)	0.53 (20)	93.3
Wood ash glass												
G9	212956	2.96 (26)	6.59 (38)	4.99 (30)	59.9 (6)	2.58 (28)	0.14 (3)	11.2 (3)	10.2 (6)	0.78 (20)	0.62 (12)	100
Wood ash lime glass												
G10	212264LG[3]	2.67 (33)	4.16 (33)	3.94 (40)	57.7 (9)	3.45 (47)	0.13 (5)	5.32 (31)	21.6 (6)	0.50 (21)	0.76 (22)	100
G11	212041	2.10 (31)	3.60 (22)	4.31 (40)	60.6 (9)	2.32 (25)	0.09 (3)	6.13 (20)	19.5 (4)	0.66 (15)	0.74 (20)	100
G12	212927	2.92 (26)	4.79 (26)	3.84 (25)	56.9 (5)	3.09 (24)	0.13 (3)	4.67 (11)	21.9 (4)	0.59 (23)	1.07 (31)	100
Mixed Alkali glass												
G13	212483	3.11 (30)	3.06 (24)	4.60 (20)	58.7 (9)	2.67 (19)	0.20 (4)	1.87 (14)	24.2 (4)	0.96 (31)	0.55 (15)	100
G14	212957	5.16 (31)	3.28 (36)	4.70 (29)	56.5 (2)	2.46 (33)	0.27 (4)	1.55 (21)	18.6 (11)	0.68 (14)	0.43 (8)	93.7
G15	272281	4.47 (24)	3.03 (21)	5.00 (22)	63.7 (4)	2.19 (40)	0.29 (4)	1.96 (23)	18.7 (5)	0.89 (11)	0.46 (23)	101
Modern-day glass												
G16	212391T[4]	13.08 (41)	0.42 (26)	2.35 (34)	69.1 (14)	0.23 (30)	0.02 (1)	0.60 (13)	9.06 (39)	0.12 (5)	0.15 (5)	95.1

Tab. 2 Summary of major and minor element compositions (in wt%) of Ribe glass by electron microprobe. Values in parentheses correspond to two SD of the mean corresponding to the trailing digits. – [1]DG = Dark green, [2]B = Blue, [3]LG = Light green, [4]T = Transparent. – (Table Museum of Southwest Jutland).

RESULTS

The chemistry of glass is controlled by its three main ingredients; the sand or pure quartz (SiO_2) making up the bulk of the glass, a flux lowering the melting temperature (typically Na, K) and a stabilizer making the glass strong and water resistant (typically Ca). The flux determines the major glass types that can be roughly divided into natron glass, plant ash glass and wood ash glass. Natron type glasses are characterized by K_2O concentrations below 2.5 wt %, plant ash glasses above 2.5 wt % and wood ash glasses by even higher concentrations of K_2O[9]. Mixed alkali glass is characterized by low K_2O concentrations, but highly elevated CaO (~20 wt %). **Figure 1** shows that of the 16 samples, 4 have K_2O and CaO corresponding to natron glass, 2 correspond to plant ash glass with K_2O around 2.5 wt % and 10 plot towards highly elevated K_2O and/or CaO concentrations (**fig. 1**). Close inspection shows that the assemblage contains glass of all three major glass types as well as a modern glass; 3 natron, 2 plant ash, 10 wood ash and 1 modern glass (**tab. 1-2**).

Natron glass

Samples G1, G2 and G3 (**tab. 1**) classify as natron type glass on the basis of their low K_2O and MgO concentrations (**tab. 2-3**). Natron glass was produced from sands at the Levantine coast or in Egypt mixed with a flux in the form of the mineral Trona ($Na_3H(CO_3)_2 \times 2H_2O$) from natron lakes in Egypt. Calcium from shells ($CaCO_3$) occurring naturally in the sands acted as stabilizer. The production of natron glass began during the Hellenistic period and continued throughout Byzantine and into Early Islamic time and can be subdivided into chemical subgroups based on slight geographical and chronological changes in recipe, raw materials and type of added compounds such as e. g. opacifiers. Based on the concentrations of SiO_2 between 63-68 wt %, Na_2O between 16-18 wt % and CaO between 7-8 wt %, samples G1, G2 and G3 classify as Roman glasses[10]. Roman glass can be further subdivided into manganese (Mn) and antimony (Sb) types produced in the Levant and Egypt, respectively. The significant chemical difference between the two groups is due to various amounts of heavy minerals rich in Al (e. g. pyroxene, feldspars, oxide minerals) in the sand sources at the two locations leading to Al_2O_3/SiO_2 ratios of 0.025-0.032 in Sb Roman glass and 0.033-0.042 in Mn Roman glass[11]. Furthermore, Roman glassmakers added Mn to the glasses at the Levantine coast and Sb to glasses produced in Egypt to reduce the natural iron in the glasses and obtain colourless glass. In primary Mn Roman glass[12], Mn range between 6200 ppm and 12,000 ppm and Sb is below 250 ppm, whereas in Sb Roman glass[13], Sb contents range between 2250 ppm and 6000 ppm while Mn contents are below 190 ppm. Most Roman glasses contain both Sb and Mn due to later recycling leading to mixing of the two types. This third subgroup is referred to as Mn-Sb Roman glass and have been defined by Sb and Mn above 250 ppm and 190 ppm, respectively[14].

Sample G1 is a transparent greenish sherd from the side of a drinking glass with Al_2O_3/SiO_2 ratio of 0.039 and Sb and Mn concentrations of 752 ppm and 2792 ppm. The Al_2O_3/SiO_2 ratio points to a Mn Roman type glass that have seen some remelting in the presence of Sb Roman glass and therefore classify as Roman Sb-Mn glass.

Samples G2 and G3 are opaque, blue chips coloured by Cu and Co (**tab. 1; tab. 3**). The high antimony (Sb) in these glasses (20,108 ppm and 16,492 ppm) were added later as opacifier and it is not possible to determine if these glasses originally had antimony. However, Al_2O_3/SiO_2 ratios of 0.037 and 0.035 indicate that these were Mn type Roman glasses possibly remelted in the presence of Sb Roman glass. Sb-Mn type Roman glass is found mainly from 1st to 3rd century AD[15].

Glass Type	Cat. No.	Na_2O wt%	MgO wt%	Al_2O_3 wt%	K_2O wt%	CaO wt%	TiO_2 wt%	MnO wt%	FeO wt%	V ppm	Cr ppm	Co ppm	Cu ppm	Zn ppm	Rb ppm	Sr ppm	Zr ppm	Nb ppm
Roman glass																		
G1	212264DG[1]	16.6	0.83	2.77	0.89	8.51	0.12	0.36	0.71	16.9	17.2	8.58	530	62.9	11.8	522	65.7	2.20
G2	212679	17.5	0.65	2.32	0.60	7.56	0.10	0.65	0.97	18.8	15.0	540	3143	132	9.20	484	58.0	1.93
G3	212391B[2]	15.5	0.69	2.33	0.74	7.14	0.10	0.46	0.93	17.2	13.4	536	2134	57.2	10.3	419	54.6	1.99
Plant ash glass																		
G4	212267	15.5	5.67	1.56	2.69	5.76	0.11	1.30	1.48	17.5	42.8	1137	2023	887	11.7	503	166	2.22
G5	212677	15.3	4.18	2.01	2.87	8.64	0.13	0.13	1.04	15.5	42.7	746	721	1159	11.1	507	74.5	2.34
Early wood ash glass																		
G6	212680	0.92	5.50	3.27	12.9	18.8	0.44	1.57	1.22	28.5	27.3	11.6	60.6	93.4	252	582	297	8.58
G7	212955	0.56	4.15	2.65	10.9	18.0	0.39	0.68	0.87	22.4	33.8	6.11	52.0	274	120	420	232	7.57
G8	212685	0.63	4.33	2.39	9.33	15.5	0.36	0.67	0.80	19.6	32.5	6.16	56.9	153	128	354	229	7.10
Wood ash glass																		
G9	212956	2.82	6.55	4.29	10.8	11.7	0.36	0.63	0.98	22.2	23.2	5.95	44.1	225	197	378	203	6.03
Wood ash lime glass																		
G10	212264LG[3]	2.54	4.11	3.39	5.06	25.1	0.24	0.76	0.72	22.2	22.8	11.5	220	272	73.3	1133	149	6.51
G11	212041	2.00	3.49	3.69	5.86	22.1	0.19	0.72	0.92	16.4	13.1	4.79	81.3	143	145	737	124	3.78
G12	212927	2.80	4.76	3.22	4.51	25.0	0.23	0.99	0.81	20.8	21.2	39.3	47.3	177	46.2	971	151	6.12
Mixed Alkali glass																		
G13	212483	3.01	2.89	3.93	1.67	27.4	0.25	0.55	1.18	19.6	21.5	4.78	51.3	281	33.6	647	214	5.73
G14	212957	4.85	2.95	4.01	1.51	22.2	0.24	0.47	1.01	19.6	20.5	5.20	23.1	174	22.6	569	181	4.64
G15	272281	4.32	2.85	4.40	1.83	21.5	0.28	0.48	1.18	22.0	24.8	5.15	20.6	166	30.5	522	242	5.73
Modern-day glass																		
G16	212391T[4]	12.7	0.10	1.65	0.53	11.1	0.03	BDL	0.04	6.33	3.74	0.34	2.81	3.54	8.43	291	106	0.91

Tab. 3 Summary of major, minor and trace element compositions (in wt% and parts per million; ppm) of Ribe glass by LA-ICPM-MS. – [1]DG = Dark green; [2]B = Blue; [3]LG = Light green; [4]T = Transparent. – (Table Museum of Southwest Jutland).

Plant ash glass

The main flux in plant ash is Na_2O but also lower concentrations of K_2O (**tab. 2-3**). Samples G4 and G5 (**tab. 1**) come from blue beads coloured by Co and Cu and classify as plant ash glass on the basis of K_2O above 2.5 wt% (**tab. 2-3**; **fig. 1**). The CaO above 5 wt% and Na_2O concentration around 15 wt% in both samples furthermore correspond to the criterias for plant ash glass although chemistry may vary depending on the local habitat[16], the exact plant species and its absorption of sodium[17]. The $^{87}Sr/^{86}Sr$ ratios for the plant ash glasses are on the order of 0.7084 (**fig. 3; tab. 4**).

Wood ash glass

Wood ash production starting around AD 780 was based on quartzite or sand with low lime mixed with wood ash (typically from beech). Wedepohl and co-authors have characterized wood ash glass production sites in Germany of known ages and found that the earliest wood ash glass had K_2O, CaO and Na_2O concentrations of 9-14 wt%, above 15 wt% and 0.9-3 wt%, respectively[18]. Over time, wood ash glass subtypes developed that can be roughly distinguished on the basis of their CaO/K_2O ratio[19]:

Early wood ash glass – from AD 780-1000 with a CaO/K_2O ratio of ≈ 1.5 (1 to 6).
Wood ash glass – from AD 1000-1400 with a CaO/K_2O ratio of ≈ 1.
Early wood ash lime glass – from AD 1300-1400 with a CaO/K_2O ratio of ≈ 1.9.
Wood ash lime glass – from AD 1300-1500 with CaO/K_2O ratio of ≈ 3.4.
Mixed alkali glass – from AD 1500 with CaO/K_2O ratio of ≈ 8.8.

Sn ppm	Sb ppm	Ba ppm	La ppm	Ce ppm	Pr ppm	Nd ppm	Sm ppm	Eu ppm	Gd ppm	Tb ppm	Dy ppm	Ho ppm	Er ppm	Tm ppm	Yb ppm	Lu ppm	Pb ppm	Bi ppm	Th ppm	U ppm
113	752	277	7.43	13.7	1.76	7.28	1.50	0.41	1.40	0.21	1.31	0.27	0.80	0.11	0.71	0.10	482	0.05	1.20	1.05
220	20108	276	7.22	12.9	1.71	6.97	1.34	0.38	1.33	0.19	1.18	0.24	0.73	0.10	0.62	0.09	15270	0.78	1.24	1.06
226	16492	297	6.77	12.2	1.58	6.35	1.28	0.35	1.25	0.18	1.12	0.23	0.69	0.10	0.60	0.09	5776	0.33	1.24	1.25
739	2.42	251	7.41	14.1	1.64	6.37	1.25	0.26	1.05	0.15	0.97	0.20	0.61	0.09	0.58	0.09	3476	0.11	1.93	0.73
442	1.35	110	7.76	15.0	1.74	6.67	1.26	0.28	1.08	0.15	0.94	0.19	0.53	0.07	0.51	0.08	3499	0.06	1.62	0.72
1.23	0.48	4315	32.0	52.7	5.34	18.9	3.03	0.56	2.75	0.41	2.51	0.53	1.65	0.24	1.62	0.25	6.28	0.01	6.32	1.66
0.70	0.33	1481	28.3	48.2	4.79	16.9	2.63	0.48	2.06	0.32	2.10	0.44	1.39	0.20	1.40	0.22	5.92	0.02	3.87	1.22
0.87	0.51	1611	42.1	67.5	7.01	23.5	3.10	0.53	2.29	0.33	2.11	0.44	1.40	0.20	1.35	0.21	10.2	0.02	4.00	1.26
1.10	0.35	1027	40.0	52.6	6.09	20.9	3.23	0.51	2.72	0.39	2.53	0.50	1.55	0.22	1.51	0.22	6.03	0.06	4.09	1.41
0.65	0.48	3132	12.6	20.8	2.32	8.47	1.64	0.38	1.51	0.21	1.34	0.29	0.87	0.12	0.87	0.13	9.47	0.03	3.25	0.93
12.9	0.66	2403		18.6	2.12	7.92	1.52	0.35	1.32	0.19	1.26	0.26	0.82	0.12	0.79	0.13	112	0.06	2.47	0.69
2.73	0.51	4908	12.4	22.7	2.58	9.60	1.80	0.43	1.59	0.24	1.51	0.30	0.96	0.12	0.94	0.14	11.3	23.0	3.47	1.08
21.9	1.15	1405	12.2	24.3	2.66	10.0	1.89	0.42	1.69	0.26	1.66	0.33	1.04	0.16	1.09	0.17	131	0.13	3.50	1.05
7.06	0.60	1512	12.6	24.5	2.83	10.7	2.04	0.42	1.86	0.27	1.70	0.35	1.05	0.15	1.04	0.16	127	0.10	3.21	0.88
4.65	0.42	1338	14.3	28.1	3.25	12.5	2.41	0.50	2.19	0.32	2.12	0.42	1.31	0.19	1.29	0.20	30.3	0.03	3.82	1.11
0.09	0.55	231	2.92	4.20	0.52	1.99	0.35	0.09	0.37	0.05	0.32	0.07	0.21	0.03	0.22	0.03	3.20	0.03	0.38	0.20

Tab. 3 (continued).

Glass Type		Cat. No.	Sr ppm	$^{87}Sr/^{86}Sr$[1]	2 sigma[2]
Plant ash glass	G4	212267	503	0.708342	0.000015
	G5	212677	507	0.708593	0.000029
Early wood ash glass	G6	212680	582	0.714546	0.000015
	G7	212955	420	0.710446	0.000036
Wood ash glass	G9	212956	378	0.716708	0.000015
Wood ash lime glass	G10	212264LG	1133	0.709069	0.000015
	G11	212041	737	0.715500	0.000015
	G12	212927	971	0.713346	0.000016
Mixed Alkali glass	G13	212483	647	0.716191	0.000021
	G15	272281	522	0.716450	0.000016

Tab. 4 Sr isotope compositions of Ribe glass by MC-ICP-MS. –

[1] All reported $^{87}Sr/^{86}Sr$ ratios represent average of 3 repeat analysis.

[2] Two sigma analytical precision determined from long-term reproducibility of SRM-987 Sr std except when sample reproducibillity exceeded this (> 0.000015). – (Table Museum of Southwest Jutland).

The change in CaO/K_2O ratio reflects an increase in CaO (to over 20 wt %) and a decrease in K_2O (from 15 to about 3 wt %) over time[20].

Early wood ash glass

The green (G6) and opaque-blue (G7, G8; **tab. 1**) beads with CaO/K_2O ratios of 1.5, 1.7 and 1.7 classify as early wood ash glass (**tab. 2-3**)[21]. The $^{87}Sr/^{86}Sr$ ratios of 0.714546 and 0.710446 for G6 and G7 are elevated and significantly different (**fig. 3; tab. 4**).

Wood ash glass

Sample G9 is a transparent greenish sherd with a CaO/K_2O ratio of 1.1 (**tab. 2-3**) that classify as wood ash glass. The $^{87}Sr/^{86}Sr$ value of 0.716708 is the highest observed (**fig. 3; tab. 4**).

Wood ash lime glass

Like sample G9, samples G10, G11 and G12 (**tab. 1**) are transparent greenish sherds (presumably window glass), but with relatively higher CaO/K_2O ratios of 5.0, 3.8 and 5.5 (**tab. 2-3**). These samples are wood ash lime glasses from around AD 1400-1600 on the basis of CaO/K_2O ratios and other major oxide systematics corresponding to observations by Wedepohl and Simon for this type of glass[22]. The elevated $^{87}Sr/^{86}Sr$ values vary from 0.709069 to 0.715500 (**fig. 3; tab. 4**).

Mixed alkali glass

Samples G13, G14 and G15 (**tab. 1**) are transparent dark green sherds with CaO/K_2O ratios ranging between 12-16.5 (**tab. 3**). They most likely classify as mixed alkali glass on the basis of their low K_2O and high CaO/K_2O ratios (**tab. 2-3**). Mixed alkali glass is a late wood ash glass type proposed by Wedepohl and Simon (2010) to have been produced solely from beech twigs and branches (= large proportion of bark)[23]. For glass from England, Meek, Henderson and Evans define mixed alkali glass as being made from e.g. kelp or another non-wood alkali source[24], but the high alkali in these do not match our observations and mixed alkali in this paper therefore refers to the type observed by Wedepohl and co-authors. Wedepohl and Kronz report high CaO/K_2O ratios around 9 for mixed alkali glass samples from the Taunus Mountains, which they relate to the low K_2O concentrations in beech bark[25]. The CaO/K_2O ratios of 12-16.5 outlined above for the Ribe samples G13, G14 and G15 are comparable to this. Alternatively, G13, G14 and G15 share many similarities with high-lime low-alkali (HLLA) type glass made from hardwood such as oak[26] and characterized by SiO_2, Na_2O and CaO concentrations around 56-61 wt %, 0-5 wt % and approximate 22 wt %[27]. According to Dungworth and Girbal[28], HLLA glasses have MgO and K_2O concentrations below 5 wt % and 10 wt % respectively and a CaO concentration above 20 wt %. Two subtypes of HLLA glasses from AD 1586-1610 and from AD 1610-1700 can be distinguished by MnO concentrations above or below 0.2 wt %. G13, G14 and G15 in our study fulfil these criteria with the exception of slightly high Na_2O concentrations. Based on this and their MnO concentrations above 0.2 wt % (**tab. 3**), they could be identified as AD 1567-1610 HLLA glasses[29]. Whether they are HLLA or mixed alkali glasses, the K_2O concentrations in these samples are lower than reported for either type although to a lower degree in the case of mixed alkali glasses. We therefore conclude that they are most likely mixed alkali type glasses presumably made from beech twigs and bark. The $^{87}Sr/^{86}Sr$ values of around 0.7163 for these samples are again highly elevated compared to plant ash and natron type glasses as is the case for all wood ash glass in this study (**tab. 4**). Generally, the wood ash samples from Ribe are furthermore characterized by high P_2O_5 (2-3.5 wt %) and Ba (> 1000 ppm) concentrations relative to Roman and plant ash type glass, whereas the MgO concentrations around 3.5 to 6 wt % are comparable to levels in plant ash glass (**tab. 2-3**)[30].

Synthetic Soda glass

Production of synthetic soda glass started in early part of the 19th century due to the discovery of synthetic soda by Nicholas Leblanc[31]. Modern soda glass can be distinguished from historical glass by the absence of chlorine as is the case for glass sample G16 from Ribe (**tab. 1-2**). Dungworth and Girbal developed a classification scheme for dividing modern glass into chronologically significant groups on the basis of P_2O_5, MgO, K_2O and As concentrations[32]. According to this, G16 classify as synthetic soda glass in production from 1870-1930[33].

DISCUSSION

Our analyses show the presence of all major glass types under the »one roof« in the about AD 850 pit house stretching in age from about the AD 200 Roman glass to the 1930 synthetic soda glass. The glass that could belong in the house include three Roman glasses, two plant ash glasses and three early wood ash glasses, whereas the glass types post-dating the house include one wood ash glass, three wood ash lime glasses, three mixed alkali glasses and one synthetic soda glass. The latter attests to a recurrent post-850 occupation of the site and re-deposition in the fill of the building through bioturbation and piping, as it was observed already during the excavation. An important conclusion from this study is thus the diversity of glass sources accessible in Ribe through import from the mid 9th century until recent times.

Natron glass

The Roman glass include one greenish transparent sherd and two blue chips coloured by copper and cobalt and with a high content of Sb from calcium antimonate ($Ca_2Sb_7O_7$ or $Ca_2Sb_2O_6$) used as opacifier (**tab. 1; tab. 3**)[34]. The sherd probably belonged to a drinking vessel, which despite its transparency contains significant amounts of colourants such as Cu, Pb and Sn. This reflects a prolonged history of recycling in the presence of coloured glass and previous studies have shown that a »substantial proportion of the glass in use in western Europe comprised recycled coloured glass«[35]. Despite the identification as a Roman period type of glass, it is thus likely that the sherd came from a vessel that was produced, used and discarded in the 9th century.

Coloured chips and tesserae were found in layers from the 8th and 9th century in Ribe, where they were used as raw material for glass beads[36]. They occur most commonly in the mid-8th century. When they are found here in the sunken-featured building from the mid-9th century it may thus either be as a raw material for a lingering glass bead production, or, perhaps more likely, as redeposited, earlier material accidentally brought down into the fill.

Plant ash glasses

The plant ash glass includes two blue beads coloured by Cu and Co and a high content of Zn and Pb (**tab. 1; tab. 3**)[37]. The beads show a striation from drawn-out air bubbles indicating that they were produced from drawn and cut-glass tubes. This is a production technique typical of imported, Middle Eastern beads, which were very common in Ribe in the first half of the 9th century[38]. Plant ash glasses are produced by quartz as pebbles or grains that are low in lime due to the natural relatively high level of Ca in halophytic plant ash[39]. Since Sr substitutes for Ca, the Sr isotopic ratio of plant ash glass therefore is controlled by the ash component, which is again controlled by the bedrock geology from which the soil formed[40]. The Sr isotope compositions of G4 and G5 correspond to Tyre 12 (a Co-blue plant ash glass from Tyre)[41], and, like Tyre 12, the samples in this study have elevated Co, Cu and Zn due to colourant addition. The $^{87}Sr/^{86}Sr$ ratio of Tyre 12 is slightly different from the other (non-coloured) Tyre glasses from that site[42], indicating the use of a different plant ash for this sample. The ε_{Nd} of -3.8 for this glass, which is higher than other Tyre samples, suggests the use of a different quartz source as well. Based on this and the resemblance of its major element composition to that of glass from the Serçe Limanı wreck, Degryse et al. conclude that this has the same origin that is presumably not Tyre. It is therefore likely that two plant ash glass beads from Ribe are of the same type. Albeit probably produced in the Middle East, the occurrence of these beads in the context of a 9th century building in Ribe is thus in good accordance with a well-documented pattern of long-distance trade[43].

Wood ash glass

The early wood ash glasses are opaque-blue (two) and green (one) beads, but there is nothing in their chemistry that can explain the colours (**tab. 1; tab. 3**). Similar opaque-blue glass fragments from the 13th century Holm Cultram Abbey in Cumbria were described and analysed by Benzonelli and Freestone[44]. These authors conclude that over-heating of the glass led to formation of tricalcium phosphate $Ca_3(PO_4)_2$ crystals resulting in blue colour and opalescence as well as an increase in the polymerization of the glass and thus its durability. These latter abilities and the presence of this bead type from other excavations in Ribe indicate that this over-heating technique was well-developed and skilfully applied during the 9th century[45]. The remainder wood ash glass and mixed alkali glass are greenish sherds. In wood ash glass, K_2O is the main flux (supplemented by addition of Na in the form of NaCl if needed), whereas high CaO content functions as stabilizer[46]. In the beginning, wood ash glass was made from beech trunks, which can have K_2O up to 12 wt % and CaO/K_2O as low as 1[47]. Later, branches and twigs (and thus a high proportion of bark with CaO/K_2O up to 16) were used as well and subtypes characterized by elevated CaO/K_2O ratios developed over time[48]. These subtypes include early wood ash, wood ash, early wood ash lime, wood ash lime and mixed alkali glass with CaO/K_2O ratios of about 1.5, 1, 2, 3.5 and 8, respectively, although the early wood ash glass varies from 1-6 (with a mean of 1.5). With the exception of early wood ash lime glass, all subtypes were present in the K4 pit house.
Wood ash glass from England and France generally have higher P_2O_5 and MgO concentrations relative to glass from the Germanic countries[49] and based on this and other chemical characteristics (see below), the wood ash glass from the K4 pit house in Ribe originate from Germanic areas.

The quartz source

As outlined above, the two primary components of natron and plant ash glasses are quartz and a flux (natron and ash of halophytic plants, respectively). In these, Rare Earth Elements (REE) from the heavy mineral assemblage in the quartz source dominate any REE contributions from the natron and saline soils that provide the substrate for halophytic plants. Wedepohl and Simon conclude the same to be the case in wood ash glass since all types have comparable concentrations of REE and other minor elements controlled by heavy minerals in sands (e.g. V and Nb)[50]. By comparing the REE patterns from glass at primary wood ash production sites with glass that arrived in trading towns such as Ribe, it thus may be possible to determine the provenance of the quartz component of the glass. Wedepohl and Simon present mean values for wood ash glass types from a number of sites in Germany[51]. **Figure 2a-c** show REE patterns normalized to continental crust for these glasses compared to the wood ash, wood ash lime and mixed alkali glasses from Ribe. The figures show that early wood ash and wood ash glass from Ribe have identical high REE concentrations and REE patterns that are enriched in Light REEs (LREE = La-Nd; **fig. 2a**), whereas the wood ash lime and mixed alkali glasses have lower concentrations and slight enrichments in the Heavy REEs (HREE = Er-Yb; **fig. 2b-c**). All wood ash glasses show Eu anomalies, reflecting the origin of the sands from weathered granites in the upper continental crust[52].

The overlap of the REE patterns for the early wood ash glasses and the wood ash glass from Ribe indicates that these are in fact all early wood ash glass. This is not unlikely given the large range in CaO/K_2O ratios observed for the early wood ash production (see result section). A similar distinct LREE enriched pattern has only previously been observed for a sample at the Carolingian Royal Palace of Paderborn (**fig. 2a;** sample Pad10 from Wedepohl and Simon[53]) and it is therefore likely that Pad10 and the Ribe early wood ash samples share the same quartz source and perhaps even production site. The similar major element chemistries furthermore suggest that a similar wood ash source was used in their production.

For wood ash lime glasses from Ribe, REE patterns and concentrations overlap with AD 1400-1600 wood ash lime glasses from Höxter, Westphalia (**fig. 2b**)[54], and could potentially have the same quartz source. Major elements also match for Höxter and Ribe wood ash lime glasses, whereas they can be clearly distinguished from the early wood ash lime glass reported by Wedepohl and Simon[55] and shown as the punctuated line in **figure 2a**.

The about AD 1450 mixed alkali glass from the Taunus Mountains proposed by Wedepohl and Simon to have been produced solely from beech twigs and branches show similar but not identical patterns with the Ribe mixed alkali glasses (**fig. 2c**)[56]. For instance, a negative Ce anomaly is not seen for the Ribe samples. It is therefore unlikely that these samples were made with the same source of sands. The low K_2O in the Taunus glasses due to bark must have required the glassmakers to add additional flux

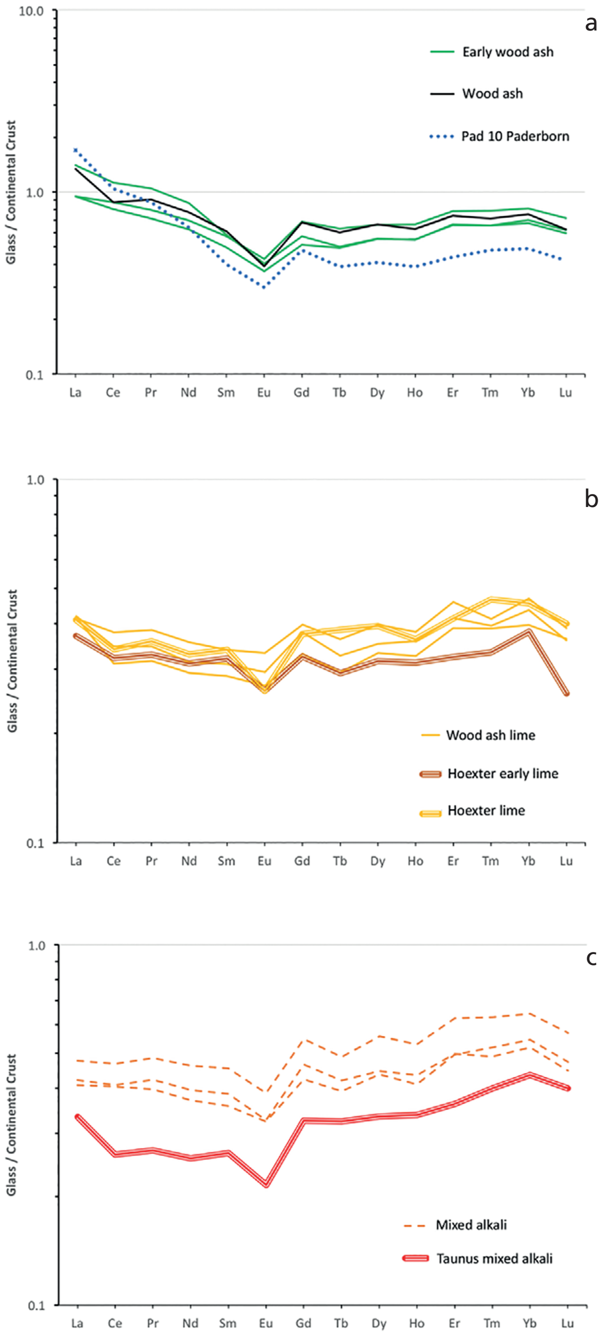

Fig. 2 Rare Earth Element (REE) patterns for glass samples from K4 pit house compared to other studies. REE concentrations were normalized to Continental Earth's crust from Wedepohl (1995). X-axis is a logarithmic scale. – **a** Early wood ash glass (green line) and wood ash glass (black line) from K4 pit house compared to mean value of 6 early wood ash glasses (double green line) from Laudengrund glass-house and 7 wood ash glasses (double black line) from Höxter, both in Germany (Wedepohl/Simon 2010). – **b** Wood ash lime glass from K4 pit house (yellow line) compared to mean value of 5 early wood ash lime glasses (double red line) and 7 wood ash lime glasses (double yellow line) from sites in Germany (Wedepohl/Simon 2010). – **c** Mixed alkali glass from K4 pit house (red dashed line) compared to mean value of 9 mixed alkali glasses (double red line) from sites in Germany (Wedepohl/Simon 2010). Data from **tab. 3**. – (Diagrams modified after Wedepohl/Simon 2010).

in the form of NaCl until a concentration of 2.5 wt % Na_2O and 5.5 wt % total alkali (K_2O+Na_2O) was reached[57]. The mixed alkali glasses from Ribe have even lower K_2O concentrations and CaO/K_2O ratios up to 16. However, the Na_2O is correspondingly higher at 3-5 wt % keeping the sum of total flux (alkali) the same as in the Taunus glasses at about 6 wt %. This strongly indicates that the starting material in the Ribe »mixed alkali glass« had the highest proportion of beech bark but that the glass-makers understood how to compensate for this by adding more NaCl to obtain enough flux to allow melting at a lower temperature.

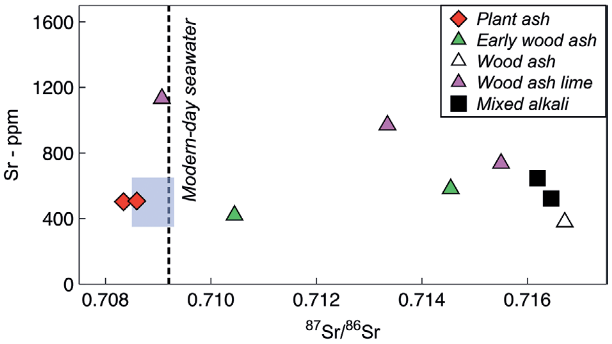

Fig. 3 Strontium concentration (ppm) versus strontium isotope ratios for glasses from pit house K4 in Ribe. Solid line shows modern day ocean water value of $^{87}Sr/^{86}Sr = 0.7092$ and shaded area represents typical compositions of natron-type glass types. Values from **tab. 4**. – (Modified after Freestone et al. 2003).

The wood ash source

Like for plant ash glass, strontium in wood ash glass follows calcium, enters the tree through uptake from the soil and is thus controlled by the local bedrock geology. When the wood is burned, Sr becomes concentrated in the ash, which has led to the high Sr concentrations up to 1100 ppm in the Ribe wood ash samples. To our knowledge this study reports the first $^{87}Sr/^{86}Sr$ ratios from wood ash glasses produced in the Germanic areas during the Middle ages. These show highly variable $^{87}Sr/^{86}Sr$ ratios that vary from 0.710446 slightly above modern seawater (= 0.7092) to highly elevated values of 0.716450 (**fig. 3**). There is no systematics between $^{87}Sr/^{86}Sr$ ratios and wood ash subtypes. On the contrary, values for early wood ash glass and wood ash lime glass cover the entire observed range, whereas mixed alkali glasses have identical, high values (**fig. 3**). It takes several tons of trees to produce one ton of wood ash and the varied values for the wood ash glasses likely reflect a mix of trees from different regional areas.

CONCLUSIONS AND PERSPECTIVES

The presence of so many distinct glass types and subtypes in a single house in Ribe is not surprising given the signs of disturbance but also the fact that many studies have documented intense glass recycling during the Middle Ages. Although the Roman sherd shows signs of recycling given its high contents of colourants, the remaining glass types do not appear to have been mixed with older glass types. This has allowed for the observation of the diversity of glass sources accessible in Ribe from the 9th century. The ability to separate the different glass types chemically enables us to confirm suspicion of intrusive finds among the artefacts. During excavation the fill layer was seen as very bioturbated, confirmed by the results of the glass analysis. The identification of Islamic plant ash glass is striking, but not unexpected given the rich occurrence of Middle Eastern coins and beads as traded objects in Viking Age Scandinavia. The occurrence of beads made of early wood ash glass is more surprising regardless of whether these were produced in Ribe or imported from elsewhere, they demonstrate an early proliferation of this new, regional glass type.

Acknowledgements

The study was supported by the Danish National Research Foundation under Grant DNFR119 – Centre for Urban Network Evolutions (UrbNet) and the Danish National Research Foundation under Grant 26-123/8 (Niels Bohr Professorship in Geoscience). We thank E. Rosenberg for help with ICP-MS data reduction and T. Ulrich and R. Andreasen for assistance during Electron Microprobe analysis and Sr isotope analysis, respectively. Discussions with I. Freestone significantly improved the manuscript.

Notes

1) See e. g. Phelps et al. 2016.

2) See e. g. Wedepohl / Simon 2010.

3) Rehren / Freestone 2015, 239.

4) Feveile / Jensen 2006.

5) Duckworth / Cuénod / Mattingly 2015.

6) For details see Hoffmann Barfod et al. 2018.

7) Weis et al. 2006.

8) Similar to 0.708989 ± 0.000013 from Hoffmann Barfod et al. 2020, but different from 0.70941 (± 0.00007) from Van Ham-Meert et al. 2018.

9) See e. g. Sayre / Smith 1961. – Werf et al. 2009. – Wedepohl / Simon / Kronz 2011.

10) See e. g. Arletti / Quartieri / Vezzalini 2006.

11) Schibille / Sterrett-Krause / Freestone 2017.

12) Referred to »high-Mn« and »Rom-Mn« by Jackson / Paynter 2016 and Schibille / Sterrett-Krause / Freestone 2017, respectively.

13) Corresponding to »Sb« and »Rom-Sb« by Jackson / Paynter 2016 and Schibille / Sterrett-Krause / Freestone 2017, respectively.

14) Schibille / Sterrett-Krause / Freestone 2017.

15) Paynter et al. 2015.

16) See e. g. Wedepohl / Simon / Kronz 2011.

17) Rehren / Freestone 2015, 237 fig. 5.

18) Wedepohl / Simon 2010. – Wedepohl / Simon / Kronz 2011.

19) Wedepohl / Simon 2010.

20) Wedepohl / Simon 2010.

21) Wedepohl / Simon 2010.

22) Wedepohl / Simon 2010.

23) Wedepohl / Simon 2010.

24) Meek / Henderson / Evans 2012.

25) Wedepohl / Kronz 2009.

26) Dungworth / Clark 2004.

27) Dungworth / Clark 2004. – Schalm et al. 2007.

28) Dungworth / Girbal 2011.

29) Dungworth / Girbal 2011, 2 fig. 1.

30) See e. g. Jackson / Smedley 2004.

31) Dungworth / Girbal 2011.

32) Dungworth / Girbal 2011.

33) Dungworth / Girbal 2011, 2 fig. 1.

34) Henderson 1985.

35) Rehren / Freestone 2015, 238.

36) Feveile / Jensen 2006, 151. – Hoffmann Barfod / Feveile / Sindbæk in press.

37) Henderson 1985.

38) Sode / Feveile / Schnell 2010.

39) Freestone / Gorin-Rosen 1999. – Barkoudah / Henderson 2006.

40) Freestone et al. 2003.

41) Degryse et al. 2010.

42) Degryse et al. 2010.

43) Callmer 1991.

44) Benzonelli / Freestone 2016.

45) Callmer 1977.

46) See e. g. Storm / Spliethoff / Hein 2000. – Wedepohl / Simon 2010. – Wedepohl / Simon / Kronz 2011.

47) Storm / Spliethoff / Hein 2000.

48) Wedepohl / Simon 2010. – Phyllis2 biomass database.

49) Jackson / Smedley 2004. – Wedepohl / Simon 2010. – Velde 2013, 74 fig. 1.4.5. – Meek / Henderson / Evans 2012.

50) Wedepohl / Simon 2010.

51) Wedepohl / Simon 2010.

52) See e. g. Taylor / McLennan 1981.

53) Sample Pad10 from Wedepohl / Simon 2010, 94 fig. 3.

54) König et al. 2002. – Wedepohl / Simon 2010.

55) Wedepohl / Simon 2010.

56) Wedepohl / Simon 2010.

57) Wedepohl / Simon 2010, 92 tab. 2.

References

Adlington 2017: L. W. Adlington, The Corning Archaeological Reference Glasses: New Values for »Old« Compositions. Papers from the Inst. of Arch. 27(1) Art. 2, 2017, 1-8.

Arletti / Quartieri / Vezzalini 2006: R. Arletti / S. Quartieri / G. Vezzalini, Glass mosaic tesserae from Pompeii: an archeometrical investigation. Periodico di Mineralogia 75(2-3), 2006, 25-38.

Barkoudah / Henderson 2006: Y. Barkoudah / J. Henderson, Plant ashes from Syria and the manufacture of ancient glass: ethnographic and scientific aspects. Journal Glass Stud. 2006, 297-321.

Benzonelli / Freestone 2016: A. Benzonelli / I. Freestone, Report on the Examination of Glass Fragments from Holm Cultram Abbey. In: Holme Cultram Abbey (GHTL14 HCA-A). Final report on archaeological excavations at Holme Cultram Abbey summer season 2014 (Wigton 2015) 110-119.

Callmer 1977: J. Callmer, Trade Beads and Bead Trade in Scandinavia, ca. 800-1000 AD. Acta Arch. Lundensia Ser. in 4°, 11 (Bonn 1977).

1991: J. Callmer, Beads as a criterion of shifting trade and exchange connections. Stud. Sachsenforsch. 7, 1991, 25-38.

Degryse et al. 2010: P. Degryse / I. Freestone / S. Jennings / J. Schneider, Technology and provenance study of Levantine plant ash glass using Sr-Nd isotope analysis. In: J. Drauschke / D. Keller (eds), Glass in Byzantium – Production, Usage, Analyses. RGZM – Tagungen 8 (Mainz 2010) 83-91.

Duckworth / Cuénod / Mattingly 2015: C. N. Duckworth / A. Cuénod / D. J. Mattingly, Non-destructive µXRF analysis of glass and metal objects from sites in the Libyan pre-desert and Fazzan. Libyan Stud. 46, 2015, 15-34.

Dungworth / Clark 2004: D. Dungworth / C. Clark, SEM-EDS analysis of Wealden Glass. Centre for Arch. Report 54, 2004, 1-15.

Dungworth / Girbal 2011: D. Dungworth / B. Girbal, Walmer Castle, Deal, Kent: Analysis of Window Glass. Research Dep. Report Ser. 2, English Heritage (Portsmouth 2011).

Feveile / Jensen 2006: C. Feveile / S. Jensen, ASR 9 Posthuset. In: C. Feveile (ed.), Det Ældste Ribe. Udgravninger på nordsiden af Ribe Å 1984-2000. Ribe Stud. 1.2. Jysk Arkæologisk Selskab, Den antikvariske Samling (Højbjerg 2006) 119-189.

Freestone / Gorin-Rosen 1999: I. C. Freestone / Y. Gorin-Rosen, The great glass slab at Bet She'arim, Israel: an early Islamic glassmaking experiment? Journal Glass Stud. 1999, 105-116.

Freestone et al. 2003: I. C. Freestone / K. A. Leslie / M. Thirlwall / Y. Gorin-Rosen, Strontium isotopes in the investigation of early glass production: Byzantine and early Islamic glass from the Near East. Archaeometry 45(1), 19-32.

Van Ham-Meert et al. 2018: A. Van Ham-Meert / S. M. Chernonozhkin / S. J. Van Malderen / T. Van Acker / F. Vanhaecke / P. Degryse, Assessment of Nanosecond Laser Ablation Multi-Collector Inductively Coupled Plasma-Mass Spectrometry for Pb and Sr Isotopic Determination in Archaeological Glass: Mass Bias Correction Strategies and Results for Corning Glass Reference Materials. Geostandards and Geoanalytical Research 42(2), 2018, 223-238.

Henderson 1985: J. Henderson, The raw materials of early glass production. Oxford Journal Arch. 4(3), 1985, 267-291.

Hoffmann Barfod / Feveile / Sindbæk in press: G. Hoffmann Barfod / C. Feveile / S. Sindbæk, Splinters to Splendours. From upcycled glass to viking beads at Ribe, Denmark. Arch. and Anthropological Scien. (in press).

Hoffmann Barfod et al. 2018: G. Hoffmann Barfod / I. C. Freestone / A. Lichtenberger / R. Raja / H. Schwarzer, Geochemistry of Byzantine and Early Islamic glass from Jerash, Jordan: Typology, recycling, and provenance. Geoarchaeology 33(6), 2018, 623-640.

2020: G. Hoffmann Barfod / I. C. Freestone / C. E. Lesher / A. Lichtenberger / R. Raja, »Alexandrian« glass confirmed by hafnium isotopes. Scien. Reports 10, 2020, 1-7.

Jackson / Paynter 2016: C. M. Jackson / S. Paynter, A Great Big Melting Pot: Exploring Patterns of Glass Supply, Consumption and Recycling in Roman Coppergate, York. Archaeometry 58(1), 2016, 68-95. https://doi.org/10.1111/arcm.12158.

Jackson / Smedley 2004: C. M. Jackson / J. W. Smedley, Medieval and post-medieval glass technology: melting characteristics of some glasses melted from vegetable ash and sand mixtures. Glass Technology 45(1), 2004, 36-42.

König et al. 2002: A. König / H. G. Stephan / K. H. Wedepohl / G. Hartmann, Mittelalterliche Gläser aus Höxter (ca. 800-1530). Archäologie, Chemie und Geschichte. Neue Ausgr. u. Forsch. Niedersachsen 23, 2002, 325-372.

Meek / Henderson / Evans 2012: A. Meek / J. Henderson / J. Evans, Isotope analysis of English forest glass from the Weald and Staffordshire. Journal Analytical Atomic Spectrometry 27(5), 2012, 786-795.

Paynter et al. 2015: S. Paynter / T. Kearns / H. Cool, / S. Chenery, Roman coloured glass in the western provinces: The glass cakes and tesserae from west Clacton in England. Journal Arch. Scien. 62, 2015, 66-81.

Phelps et al. 2016: M. Phelps / I. C. Freestone / Y. Gorin-Rosen / B. Gratuze, Natron glass production and supply in the late antique and early medieval Near East: The effect of the Byzantine-Islamic transition. Journal Arch. Scien. 75, 2016, 57-71.

Rehren / Freestone 2015: T. Rehren / I. C. Freestone, Ancient glass: from kaleidoscope to crystal ball. Journal Arch. Scien. 56, 2015, 233-241.

Sayre / Smith 1961: E. V. Sayre / R. W. Smith, Compositional categories of ancient glass. Science 133(3467), 1961, 1824-1826.

Schalm et al. 2007: O. Schalm / K. Janssens / H. Wouters / D. Caluwe, Composition of 12th to 18th century window glass in Belgium: Non-figurative windows in secular buildings and stained-glass windows in religious buildings. Spectrochimica Acta B 62, 2007, 663-668.

Schibille / Sterrett-Krause / Freestone 2017: N. Schibille / A. Sterrett-Krause / I. C. Freestone, Glass groups, glass supply and recycling in Late Roman Carthage. Arch. and Anthropological Scien. 9(6), 2007, 1223-1241.

Sode / Feveile / Schnell 2010: T. Sode / C. Feveile / U. Schnell, An investigation on segmented, metal-foiled glass beads and blown, mirrored glass beads from Ribe, Denmark. In: C. Theune-Vogt / F. Biermann / R. Struwe / G. H. Jeute (eds), Zwischen Fjorden und Steppe. Festschrift für Johan Callmer zum 65. Geburtstag. Internat. Arch. Stud. honoraria 31 (Rahden / Westf. 2010) 319-328.

Storm / Spliethoff / Hein 2000: C. Storm / H. Spliethoff / K. R. G. Hein, Generation of a gaseous fuel by gasification or pyrolysis of biomass for use as reburn gas in coal-fired boilers. Proceedings 5th European Conference on Industrial Furnaces and Boilers 1 (o. O. 2000) 689-699.

Taylor / McLennan 1981: S. R. Taylor / S. M. McLennan, The composition and evolution of the continental crust: rare earth element evidence from sedimentary rocks. Phil. Transactions of the Royal Soc. London A, 301(1461), 1981, 381-399.

Velde 2013: B. Velde, Glass compositions over several millennia in the western world. Modern Methods for Analysing Arch. and Hist. Glass 1, 2013, 67-78.

Wedepohl 1995: K. H. Wedepohl, The composition of the continental crust. Geochimica et Cosmochimica Acta 59(7), 1995, 1217-1232.

Wedepohl / Kronz 2009: K. H. Wedepohl / A. Kronz, Die Glas-Zusammensetzung dreier spätmittelalterlicher Hütten auf dem Taunus-Kamm unweit Glashütten. Ber. Komm. Arch. Landesforsch. Hessen 9, 2009, 135-151.

Wedepohl / Simon 2010: K. H. Wedepohl / K. Simon, The chemical composition of medieval wood ash glass from central Europe. Chemie der Erde 70(1), 2010, 89-97.

Wedepohl / Simon / Kronz 2011: K. H. Wedepohl / K. Simon / A. Kronz 2011, The chemical composition including the Rare Earth Elements of the three major glass types of Europe and the Orient used in late antiquity and the Middle Ages. Archaeometry 53(1), 2011, 81-102.

Weis et al. 2006: D. Weis / B. Kieffer / C. Maerschalk / J. Barling / J. de Jong / G. A Williams / A. Goolaerts, High-precision isotopic characterization of USGS reference materials by TIMS and MC-ICP-MS. Geochemistry, Geophysics, Geosystems 7(8), 2006, 1-30.

Werf et al. 2009: I. V. D. Werf / A. Mangone / L. C. Giannossa / A. Traini / R. Laviano / A. Coralini / L. Sabbatini, Archaeometric investigation of Roman tesserae from Herculaneum (Italy) by the combined use of complementary micro-destructive analytical techniques. Journal Arch. Scien. 36, 2009, 2625-2634.

Zusammenfassung

Geochemische und Strontium-Isotopen-Analysen mittels Mikrosonde sowie Laserablation (LA) und Multikollektor-ICP-Massenspektrometrie (MC) von 16 Gläsern aus einem Grubenhaus aus der Mitte des 9. Jahrhunderts in der Handelsstadt Ribe zeigen eine Gruppe von 3 Natrongläsern (2 blaue Späne und 1 transparente Scherbe), 2 Pflanzenaschegläsern (blaue Perlen), 3 frühe Holzaschegläser (opak-blaue Perlen), 1 Holzascheglas (Scherbe), 3 Holzasche-Kalk-Gläser (Scherben), 3 gemischte Alkaligläser (Scherben) sowie 1 »modernes« synthetisches Sodaglas (Scherbe). Die Gläser, die aus der Zeit nach dem Haus stammen, bestätigen die stratigraphischen Hinweise auf Störungen durch biologische Aktivitäten und den Aushub von Rohrleitungen. Hauptelemente, REE-Systematik und Sr-Isotope zeigen, dass das Natronglas vom römischen Typ ist, das Pflanzenascheglas wahrscheinlich aus dem islamischen Raum und das Holzascheglas aus germanischen Gebieten stammt. Die REE-Muster, die die Quarzquelle für 1. frühe Holzaschegläser und 2. jüngere Holzasche-Subtypen zurückverfolgen, sind deutlich unterschiedlich und durch LRE- bzw. moderate HRE-Anreicherungen gekennzeichnet. Die Muster passen zu Proben aus der Glashütte Laudengrund, Spessart (frühes Holzascheglas) und aus Höxter, Westfalen (Holzasche-Kalk-Glas). Die für germanische Holzaschegläser berichteten Sr-Isotopenzusammensetzungen weisen auf die Holzaschekomponente (Boden) hin und zeigen sehr unterschiedliche und erhöhte $^{87}Sr/^{86}Sr$-Verhältnisse von 0,709-0,717, ähnlich wie die berichteten Werte für Holzaschegläser aus England. Gläser aus Pflanzenasche zeichnen sich durch niedrigere $^{87}Sr/^{86}Sr$-Verhältnisse aus, die einer in Tyre beobachteten Zusammensetzung entsprechen. Die Glastypen zeugen von der Vielfalt der in Ribe ab dem 8. Jahrhundert zugänglichen Glasquellen.

Summary

Geochemical and strontium isotope analysis by microprobe as well as laser ablation (LA) and multi-collector (MC) ICP mass spectrometry of 16 glasses from a mid-9th century pit house in the emporium town of Ribe show an assemblage of 3 natron (2 blue chips and 1 transparent sherd), 2 plant ash (blue beads), 3 early wood ash (opaque-blue beads), 1 wood ash (sherd), 3 wood ash lime (sherds), 3 mixed alkali (sherds) glasses as well as 1 »modern« synthetic soda glass (sherd). The glass types post-dating the house confirm the field stratigraphic indications of disturbance from bioturbation and piping excavation. Major elements, REE systematics and Sr isotopes show the natron glass to be Mn Roman type, the plant ash glass most likely Islamic and the wood ash glass to originate from Germanic areas. REE patterns tracing the quartz source for 1. early wood ash glasses and 2. younger wood ash subtypes are distinctly different and characterized by LRE and moderate HRE enrichments, respectively. The patterns match samples from the Laudengrund glass-house, Spessart Mountains (early wood ash glass) and from Höxter, Westphalia (wood ash lime glass). The Sr isotope compositions reported for Germanic wood ash glass traces the wood ash (soil) component and show highly

varied and elevated $^{87}Sr/^{86}Sr$ ratios of 0.709-0.717 similar to reported values for wood ash glasses from England. Plant ash glasses are characterized by lower $^{87}Sr/^{86}Sr$ ratios corresponding to a composition observed at Tyre. The glass types attest to the diversity of glass sources accessible in Ribe from the 8th century and forward.